

MobileLLM-R1: Exploring the Limits of Sub-Billion Language Model Reasoners with Open Training Recipes

Changsheng Zhao^{1,*}, Ernie Chang^{1,*,\\$}, Zechun Liu^{1,*,\dagger}, Chia-Jung Chang¹, Wei Wen¹, Chen Lai¹, Sheng Cao¹, Yuandong Tian¹, Raghuraman Krishnamoorthi¹, Yangyang Shi¹, Vikas Chandra¹

¹Meta AI

*Equal contribution, authors listed in alphabetical order

\\$Led overall data curation efforts

\daggerCorresponding Author

The paradigm shift in large language models (LLMs) from instinctive responses to chain-of-thought (CoT) reasoning has fueled two prevailing assumptions: (1) reasoning capabilities only emerge in sufficiently large models, and (2) such capabilities require training on massive datasets. While the first assumption has already been challenged by recent sub-billion-parameter reasoning models such as Qwen3-0.6B and DeepSeek distilled variants, the second remains largely unquestioned. In this work, we revisit the necessity of scaling to extremely large corpora (>10 T tokens) for reasoning emergence. By carefully curating and resampling open-source datasets that we identify as beneficial under our designed metrics, we demonstrate that strong reasoning abilities can emerge with far less data. Specifically, we show that only ~ 2 T tokens of high-quality data are sufficient, and pre-training with 4.2T tokens on the dataset resampled from these ~ 2 T tokens, followed by a established post-training procedure, enables the development of MobileLLM-R1, a series of sub-billion-parameter reasoning models that substantially outperform prior models trained on fully open-sourced data. For example, MobileLLM-R1-950M achieves an AIME score of 15.5, compared to just 0.6 for OLMo-2-1.48B and 0.3 for SmoLM-2-1.7B. Remarkably, despite being trained on only 11.7% of the tokens compared to Qwen3's proprietary 36T-token corpus for pretraining, MobileLLM-R1-950M matches or surpasses Qwen3-0.6B across multiple reasoning benchmarks. To facilitate further research in this direction, we have released the complete training recipe, data sources, data mixing ratio, and model checkpoints, together with the key insights obtained throughout this study.

Date: September 30, 2025

Correspondence: Zechun Liu at zechunliu@meta.com

Author emails: {cszhao, erniecy, zechunliu}@meta.com

HuggingFace: <https://huggingface.co/collections/facebook/mobilellm-r1-68c4597b104fac45f28f448e>

Code: <https://github.com/facebookresearch/MobileLLM-R1>



1 Introduction

Large language models (LLMs) such as GPT (Achiam et al., 2023), Qwen (Yang et al., 2025, 2024), and DeepSeek (Guo et al., 2025) have demonstrated remarkable progress in explicit reasoning. Advances have been driven by scaling model size, expanding training data, and applying post-training techniques such as supervised fine-tuning (SFT) and reinforcement learning (RL). Reasoning LLMs are capable of tackling complex problems by following long chains of thought that incorporate reflection, backtracking, and self-validation. At the same time, reasoning traces have evolved from prompt-based chain-of-thought (CoT) in-context learning (Wei et al., 2022) to models explicitly optimized on long reasoning traces to generate multi-step reasoning sequence (Jaech et al., 2024).

However, this paradigm poses increasing challenges for real-world deployment. Large models already strain resource-constrained devices (Liu et al., 2024), and long-context reasoning further exacerbates memory usage as KV cache growth sharply increases the footprint (Sadhukhan et al., 2025). Looking ahead, one can envision

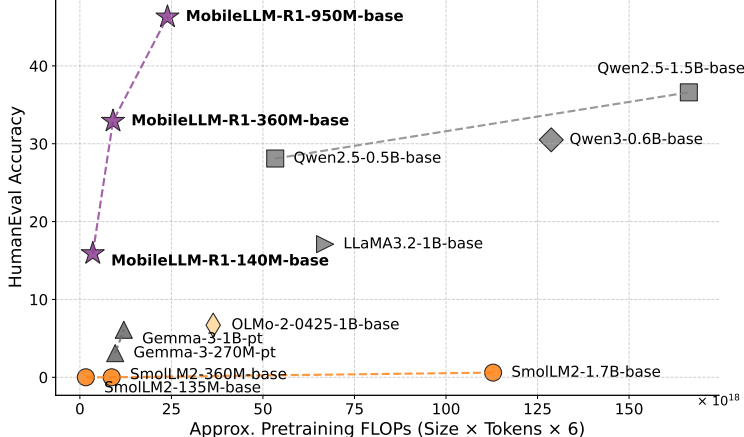


Figure 1 Pretrained model accuracy vs. training efficiency trade-off.

a future with personal assistants, smart homes, and robots increasingly relying on on-device reasoning for complex tasks. In such a world, deployability and portability will become inevitable trends for the next generation of LLMs. This motivates our central question: *Given strict capacity constraints, what is the most effective recipe to endow small reasoning models with strong capabilities and unlock their hidden potential?*

Developing small reasoning models poses unique challenges beyond simply scaling down large ones. For large models, expanding the corpus often drives stronger generalization. In contrast, small language models are far more sensitive: noise in the data can easily overwhelm their limited capacity, making data quality and curation paramount. As models shrink, neurons must encode more overlapping knowledge, increasing the risk of interference and conflicts (Zhu et al., 2025)—superposition provides an intuitive lens for understanding this challenge (Elhage et al., 2022). Mitigating these risks requires carefully optimized data, objectives, and training procedures.

While extensive research has explored how post-training objectives and data curation can elicit reasoning from pretrained models (Wang et al., 2025; Li et al., 2025), far less attention has been paid to a more fundamental question: *How can we endow pretrained models with the latent potential for reasoning in the first place?* This work addresses this gap by investigating two critical questions: (1) What kinds of data are most effective for instilling reasoning capability, and (2) How can diverse forms of reasoning—such as coding, mathematics, and logical problem-solving—be embedded into a compact model without overwhelming its limited capacity?

Through capability-aware data curation and probing into the latent factors that govern reasoning, we achieve highly token-efficient pretraining compared to prior work. With only 4.2T training tokens, just 11.7% of Qwen’s 36T, our MobileLLM-R1-950M model, matches or surpasses Qwen3-0.6B (Yang et al., 2025) on multiple reasoning benchmarks, placing itself on the Pareto frontier of accuracy-training-token efficiency trade-off curve (Figure 1). Beyond introducing a high-performing small-scale reasoning model, we share both the insights and the pitfalls encountered along the way, offering a first-hand glimpse into the complex yet fascinating mechanisms behind reasoning models.

We make the following contributions toward building the most accurate fully open-source sub-billion-parameter language model reasoners to date from scratch:

- We introduce benchmark-free, self-evolving data optimization for pre-training data curation, a principled dataset-level weighting approach that leverages cross-domain influences to tailor the data mixture. This facilitates robust reasoning generalization on held-out benchmarks, achieved without exposing them during training or data mixture optimization.
- We further propose a data–model co-evolution strategy to adapt to rapid changes in model capacity during mid-training. We show that this process converges as most samples reach zero or negative influence, indicating that the dataset’s information has been largely exhausted and offers minimal further improvement.

- Compared to existing fully open-source models, MobileLLM-R1-950M model attains $5\times$ higher MATH accuracy than Olmo 1.24B (Allal et al., 2025) and $2\times$ higher than SmoLMLM 1.7B (Allal et al., 2025), while significantly outperforming both on code benchmarks despite having fewer parameters. Comparative results are presented in Figures 2 and 3.
- We have disclosed the complete set of open-sourced datasets employed in our study and have released all trained models and accompanying code to enable full reproducibility and foster future research.

2 How do LLMs gain reasoning capability?

Previous work have studied how SFT and RL affect model's reasoning capability (Wang et al., 2025; Li et al., 2025). However, if people agree that the reasoning capability is "elicited" in the SFT/RL stages, then *how does it gain initially when it is trained from scratch?* To the best of our knowledge, there is no prior work answering that.

Large Language Models (LLMs) can be fundamentally understood as *context-conditioned pattern reconstruction*

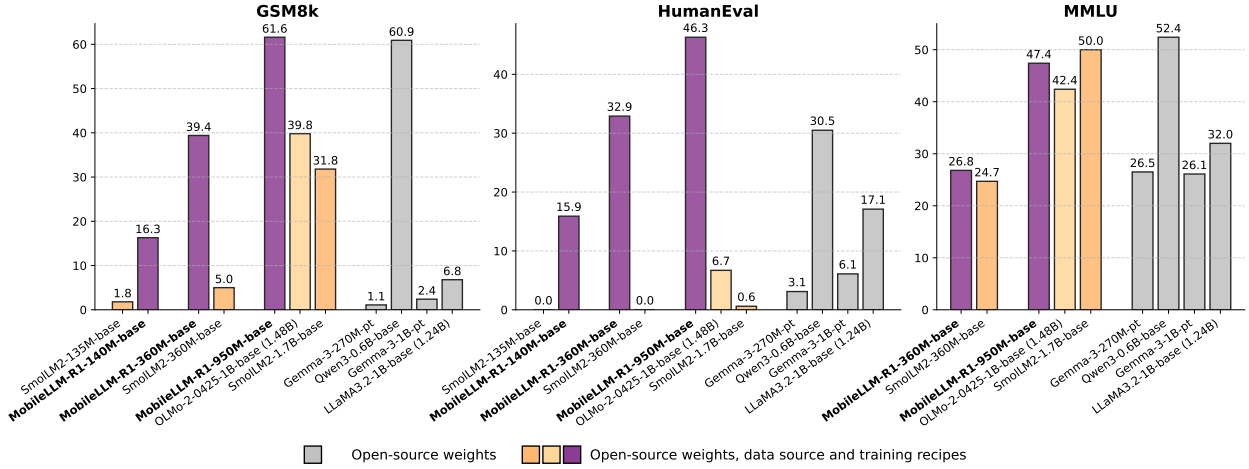


Figure 2 Performance comparison of **base models** across three tasks: GSM8k, HumanEval, and MMLU. Models are grouped by parameter size and color-coded by model family: MobileLLM-R1 (purple), SmoLMLM (orange), OLMo (yellow), and other partially open-source models (gray). Labels indicate model name and size for select models. MobileLLM-R1 consistently achieves strong performance across tasks while remaining parameter-efficient. A comprehensive comparison is presented in Table 6.

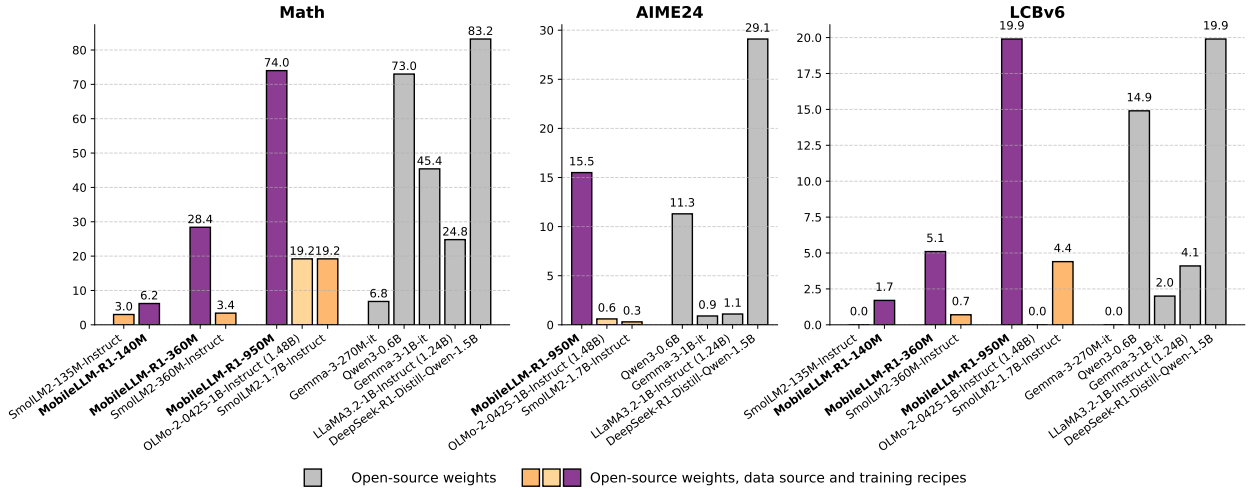


Figure 3 Performance comparison of **post-trained models** across three tasks: MATH, AIME'24, and LiveCodeBench-v6. The full comparison results are provided in Table 7.

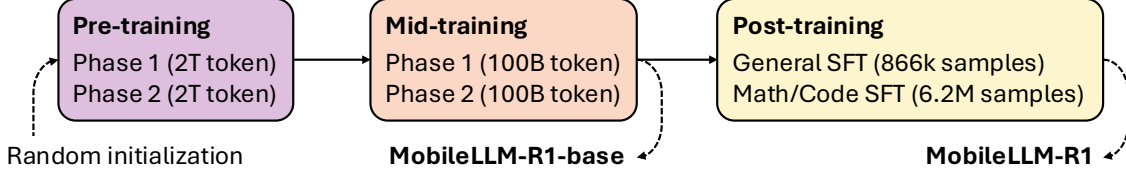


Figure 4 Overall training pipeline of MobileLLM-R1.

systems, where the central objective is to model the conditional probability distribution of the next token given its preceding context. This perspective frames LLM training as the process of refining a predictive distribution over the vocabulary space: learning, from large-scale data, the statistical regularities that govern natural language.

From this lens, the transition from a general-purpose LLM to a reasoning-specialized model can be interpreted as a systematic shift in token probability mass. That is, reasoning ability emerges not from an entirely new modeling paradigm, but from a redistribution of probability towards reasoning-relevant continuations when presented with certain contexts. Understanding this shift, both qualitatively and quantitatively, provides a principled way to study how reasoning capability is acquired.

We therefore design a complete training curriculum for building a reasoning-capable LLM from scratch, structured to deliberately guide the model through this probability-space transformation. Our approach parallels well-established principles in educational psychology: just as human learners first undergo a broad-based general education before pursuing domain-specific expertise. We found that a solid knowledge foundation is crucial for language models to stabilize their output and ensure good quality in the subsequent reasoning benchmarks.

In the **pre-training** stage, the model is first exposed to a diverse corpus that grounds it in human language and general world knowledge. During this stage, it also acquires basic mathematical and reasoning capabilities. We will later show that it is crucial to (1) include both types of data and (2) train them jointly: (1) web data provides fundamental linguistic grounding without divergence, while (2) math data develops reasoning capacity. This stage establishes a robust linguistic and conceptual foundation, enabling coherent next-token prediction across a wide range of inputs.

In the subsequent **mid-training** stage, we strategically shift the data distribution towards reasoning-rich domains such as mathematics, coding, and structured problem solving. This induces a gradual reallocation of probability mass towards reasoning-oriented continuations—analogous to how specialized education shapes cognitive priors in humans.

Finally, **supervised fine-tuning (SFT)** serves to align the model with human-preferred behaviors, equipping it with instruction-following capabilities and extended sequence handling. This final stage ensures that the reasoning ability acquired during earlier phases is accessible, controllable, and usable in practical interaction settings.

3 Final Recipe

To ensure reproducibility and to provide a transparent foundation for future research, we begin by detailing our model architecture and training setup, including the curated data sources and the complete recipe. Building upon fully open-source data, MobileLLM-R1 establishes a new standard among transparent reasoning models, achieving substantially higher accuracy than prior fully open-source efforts such as OLMo and SmoLLM.

3.1 Model Architecture

Our model architecture is based on designs from MobileLLM (Liu et al., 2024) and LLaMA3.2 (Dubey et al., 2024). We adopt the LLaMA3.2 tokenizer with a 128k subword vocabulary. We also incorporate QK-norm to mitigate training instabilities in the self-attention block. Following MobileLLM, we adopt weight sharing

between the input and output embeddings to improve parameter efficiency. A complete set of architectural specifications is reported in Table 1.

Table 1 Detailed architecture specifications of MobileLLM-R1. "Dim" denotes the embedding dimension and "Hidden Dim" represents the dimension inside the feed-forward network.

Model	Layer	Head	KV-Head	Dim	Hidden Dim	Params
MobileLLM-R1-140M	15	9	3	576	2048	140.2M
MobileLLM-R1-360M	15	16	4	1024	4096	359.4M
MobileLLM-R1-950M	22	24	6	1536	6144	949.2M

3.2 Training Recipe

The complete set of training hyperparameters is detailed in Table 2, with stage-specific configurations as follows:

Pre-training phase: Models are initialized from scratch and optimized with Adam $(\beta_1, \beta_2, \epsilon) = (0.9, 0.95, 10^{-8})$ and weight decay 0.1. The learning rate employs a 2k-step warmup followed by linear decay to $0.1 \times$ the peak value.

Mid-training phase: Optimization continues with Adam, where the learning rate decays linearly to zero. Knowledge distillation is applied with Llama-3.1-8B-Instruct model as the teacher, where the student is trained by minimizing the KL divergence between its output logits and the teacher's logits.

Post-training phase: Adam is used with zero weight decay. The learning rate warmup ratio is set to 0.03 for general-purpose SFT and 0.1 for reasoning-specific SFT, followed by linear decay to zero.

Table 2 Training setup across different stages.

Stage	Phase	Tokens / Samples	BS	Seq. Len.	Steps / Epochs	LR	#GPUs	Time
<i>Pre-training</i>	Phase 1	2T tokens	16	2k	500k	4.00E-03	16×8	4–5 days
	Phase 2	2T tokens	16	2k	500k	4.00E-03	16×8	4–5 days
<i>Mid-training</i>	Phase 1	100B tokens	4	4k	50k	3.60E-04	16×8	1–2 days
	Phase 2	100B tokens	4	4k	50k	3.60E-04	16×8	1–2 days
<i>Post-training</i>	General SFT	866K samples	4	4k	2 epoch	5.00E-06	16×8	~2h
	Reasoning SFT	6.2M samples	8	32k	4 epoch	8.00E-05	16×8	~2.5 days

3.3 Data

3.3.1 Pretraining

To balance general language understanding with strong reasoning capabilities, we design a two-stage pre-training curriculum with carefully curated data sources (Table 3). Phase 1 emphasizes broad coverage through large-scale web and educational corpora such as FineWeb-Edu, which provide linguistic and domain diversity. At the same time, we seed the mixture with reasoning-rich corpora, including OpenWebMath, Arxiv, and StackExchange, to expose the model early to mathematical and scientific discourse. In Phase 2, we deliberately shift the weighting toward specialized reasoning datasets—such as FineMath, OpenWebMath, Algebraic Stack, and Facebook Natural Reasoning—while reducing the proportion of generic sources. This skewed allocation ensures that the model continues to benefit from general pre-training signals while increasingly focusing on structured reasoning tasks, ultimately aligning the training distribution with our goal of developing a compact yet strong reasoning model. The total token count of the datasets used in per-training is 1.8T. We sample data from each source according to the predefined mixture weights, drawing a total of 2T tokens per phase.

3.3.2 Mid-training

For mid-training, we construct a mixture that complements pre-training by targeting benchmarks and reasoning-intensive domains (Table 4). The first phase emphasizes coverage of general-purpose datasets (e.g., Dolmino DCLM baseline, FLAN, and peS2o) alongside curated knowledge sources such as Wiki and

Table 3 Pre-training datasets and mixture ratios for the two-stage curriculum, with 2T tokens sampled per phase.

Dataset	Rows	Tokens (B)	Phase1 Mix	Phase2 Mix
StarCoder	206,640,114	263.8	10.66%	0.52%
OpenWebMath	6,117,786	12.6	6.93%	23.33%
FineWeb-Edu	1,279,107,432	1300	63.75%	54.83%
Wiki	7,222,303	3.7	5.03%	0.14%
Arxiv	1,533,917	28	6.36%	1.32%
StackExchange	29,249,120	19.6	5.03%	0.86%
Algebraic stack	3,404,331	12.6	2.25%	1.26%
Nemotron science	708,920	2	—	0.03%
Nemotron code	10,108,883	16	—	0.72%
Nemotron math	22,066,397	15	—	3.01%
Cosmopedia	31,064,744	25	—	2.70%
Facebook natural reasoning	1,145,824	1.8	—	3.18%
FineMath	48,283,984	34	—	8.01%
peS2o	38,800,000	50	—	0.08%
Total			100%	100%

StackExchange. This configuration is intended to improve the model’s broad knowledge, reflected in the performance in general benchmarks like MMLU, where factual recall is critical. In the second phase, we deliberately skew the mixture toward math and coding corpora, particularly Dolmino Math, Nemotron-CC-Math, and Nemotron-Code, while reducing the weight of general-purpose datasets. We also introduce a small but targeted set of benchmark-style datasets (e.g., GSM8K, ARC, OBQA) to align training with downstream evaluation. This two-stage weighting scheme allows the model to first consolidate broad knowledge and language understanding before specializing on reasoning-intensive math and code tasks, which are central to our objective of building compact yet competitive reasoning models. The reported data mix ratios correspond to post sub-sampling. We will also release the code for the sub-sampling procedure to ensure full reproducibility for anyone following our protocol. For each mid-training phase, we sample 100B tokens from the sources following the predefined mixture distribution.

Table 4 Mid-training datasets and mixture ratios, with 100B tokens sampled per phase according to the mix ratio.

Dataset	Subset	Rows (M)	Phase1 Mix	Phase2 Mix
Dolmino	DCLM Baseline	606	37.03%	6.51%
	FLAN	57.3	4.10%	0.72%
	peS2o	38.8	11.41%	2.01%
	Wiki	6.17	2.66%	0.47%
	StackExchange	2.48	2.12%	2.00%
	Math	21	11.63%	29.10%
Nemotron	Nemotron-Pretraining-Code-v1	882	20.69%	29.10%
	Nemotron-CC-Math-v1	144	3.45%	19.40%
StarCoder	StarCoder	206	6.90%	9.70%
Benchmark Set	TriviaQA (train)			
	OBQA (train)			
	NaturalQuestions (train)			
	PIQA (train)			
	GSM8K (train)	~0.01	—	0.97%
	BoolQ (train)			
	ARC-Easy (train)			
	ARC-Challenge (train)			
Total			100.00%	100.00%

3.3.3 Post-training

In the post-training stage, we leverage established post-training datasets. Following standard practice, we first align the model with instructions through general supervised fine-tuning (SFT) and then apply reasoning-specific SFT to extend the context length and promote a long chain-of-thought (CoT) reasoning style. The

datasets used in post-training are shown in Table 5

Table 5 Post-training data.

Stage	Dataset	Rows
General	Tulu3-SFT	866K
Reasoning	OpenMathReasoning	3.2M
	OpenScienceReasoning-2	802K
	OpenCodeReasoning-2	2.2M

4 Final Results

In the following, we position our trained MobileLLM-R1 within the context of prior state-of-the-art models and compare their performance. We present results for two sets of models: the base models, evaluated after pre-training and mid-training, and the final models after the complete training pipeline. The experimental settings and full training pipeline can be found in Section 3

Base Model Table 6 compares base reasoning models across multiple benchmarks. We group them into fully open-source models (OLMo (OLMo et al., 2024), SmoLLM (Allal et al., 2025), MobileLLM-R1), with weights, data, and training recipes available, and partially open-source models (Qwen (Yang et al., 2025), Gemma (Team et al., 2025), LLaMA (Dubey et al., 2024)), which released model weights and partial training procedures. Compared to fully open-source models, MobileLLM-R1 consistently outperforms both OLMo and SmoLLM across all parameter scales. For example, at the 140M scale, MobileLLM-R1 achieves 16.3% GSM8K and 15.9% HumanEval, dramatically surpassing SmoLLM2-135M (1.8% and 0.0%, respectively). Compared to prior partially open-source models, such as Qwen3-0.6B, MobileLLM-R1 achieves comparable or superior results despite being trained on substantially fewer tokens (4.2T for MobileLLM-R1 vs. 36T for Qwen3). Notably, MobileLLM-R1-950M attains the highest HumanEval score (46.3%) among all sub-1B models, significantly outperforming Qwen3-0.6B (30.5%).

Post-trained Model Table 7 presents the performance of post-trained models. Notably, on LiveCodeBench, small models below 400M parameters struggle to produce reliable outputs. In contrast, MobileLLM-R1-360M achieves 5.1 points, surpassing even models with over 1B parameters, such as SmoLLM2-1.7B, Gemma3-

Table 6 Performance comparison of reasoning base models across multiple benchmarks. Here, CommonSense Avg. denotes an average of 8 tasks in CommonSense Reasoning benchmarks including ARC-easy, ARC-challenge, BoolQ, PIQA, SIQA, HellaSwag, OBQA, and WinoGrand. Per-task accuracies are reported in Table 13. Models with fewer than 150M parameters do not yield reliable MMLU scores and are therefore denoted as ‘-’.

Model	Size	MATH500 (4-shot, em)	GSM8K (8-shot, em)	MBPP (3-shot, pass@1)	HumanEval (0-shot, pass@1)	CommonSense (0-shot, avg acc.)	MMLU (5-shot, acc.)
<i><150M</i>							
SmoLLM2-135M	135M	0.4	1.8	3.8	0.0	50.7	—
MobileLLM-R1-140M-base	140M	4.6	16.3	5.4	15.9	44.3	—
<i>150M – 400M</i>							
Gemma-3-270M-pt	268M	0.6	1.1	2.0	3.1	48.4	26.5
SmoLLM2-360M	362M	1.8	5.0	19.4	0.0	56.6	24.7
MobileLLM-R1-360M-base	359M	13.4	39.4	20.8	32.9	51.0	26.8
<i>400M – 1B</i>							
Qwen2.5-0.5B	494M	14.8	41.8	29.6	28.1	52.3	47.5
Qwen3-0.6B-Base	596M	29.8	60.9	39.0	30.5	55.3	52.4
MobileLLM-R1-950M-base	949M	26.8	61.6	39.2	46.3	58.6	47.4
<i>>1B</i>							
Gemma-3-1B-pt	1.00B	0.6	2.4	9.4	6.1	57.3	26.1
LLaMA3.2-1B	1.24B	1.6	6.8	26.6	17.1	58.4	32.0
OLMo-2-0425-1B	1.48B	5.2	39.8	7.8	6.7	61.0	42.4
Qwen2.5-1.5B	1.54B	31.0	68.4	44.6	36.6	58.7	61.2
SmoLLM2-1.7B	1.71B	11.6	31.8	35.4	0.6	62.9	50.0
Qwen3-1.7B-Base	2.03B	38.5	76.2	56.4	47.6	60.9	62.1

Table 7 Evaluation results of different reasoning models across MATH500, GSM8K, AIME’24, AIME’25, and LCBv6 benchmarks. For AIME, we evaluate models across 64 runs and report the average accuracy. For LiveCodeBench, results are reported as the average accuracy across 16 runs. Models with fewer than 400M parameters do not produce reliable AIME scores and are therefore denoted as ‘-’.

Name	Size	MATH500		GSM8K		AIME’24		AIME’25		LCBv6	
		0-shot pass@1	0-shot pass@1	0-shot pass@1	0-shot pass@1	0-shot pass@1, n=64	0-shot pass@1, n=64	0-shot pass@1, n=64	0-shot pass@1, n=64	0-shot pass@1, n=16	0-shot pass@1, n=16
<i><150M</i>											
SmolLM2-135M-Instruct	135M	3.0	2.4	—	—	—	—	—	—	0.0	
MobileLLM-R1-140M	140M	6.2	4.1	—	—	—	—	—	—	1.7	
<i>150M – 400M</i>											
Gemma-3-270M-it	268M	6.8	8.4	—	—	—	—	—	—	0.0	
SmolLM2-360M-Instruct	362M	3.4	8.1	—	—	—	—	—	—	0.7	
MobileLLM-R1-360M	359M	28.4	24.5	—	—	—	—	—	—	5.1	
<i>400M – 1B</i>											
Qwen2.5-0.5B-Instruct	494M	31.2	48.1	0.1	—	0.3	—	—	—	3.6	
Qwen3-0.6B	596M	73.0	79.2	11.3	—	17.0	—	—	—	14.9	
MobileLLM-R1-950M	949M	74.0	67.5	15.5	—	16.3	—	—	—	19.9	
<i>>1B</i>											
Gemma-3-1B-it	1.00B	45.4	62.9	0.9	—	0.0	—	—	—	2.0	
LLaMA3.2-1B-Instruct	1.24B	24.8	38.8	1.1	—	0.2	—	—	—	4.1	
OLMo-2-0425-1B-Instruct	1.48B	19.2	69.7	0.6	—	0.1	—	—	—	0.0	
OpenReasoning-Nemotron-1.5B	1.54B	83.4	76.7	49.7	—	40.4	—	—	—	28.3	
DeepSeek-R1-Distill-Qwen-1.5B	1.54B	83.2	77.3	29.1	—	23.4	—	—	—	19.9	
Qwen2.5-1.5B-Instruct	1.54B	54.0	70.0	2.5	—	0.9	—	—	—	7.9	
SmolLM2-1.7B-Instruct	1.71B	19.2	41.8	0.3	—	0.1	—	—	—	4.4	
Qwen3-1.7B	2.03B	89.4	90.3	47.0	—	37.0	—	—	—	29.8	

1B, and LLaMA3.2-1B. Remarkably, MobileLLM-R1-950M demonstrates a substantial accuracy gain over Qwen3-0.6B on LiveCodeBench and even matches the performance of much larger state-of-the-art models, such as DeepSeek-R1-Distill-Qwen-1.5B. Across Math and AIME benchmarks, MobileLLM-R1 consistently outperforms other fully open-source models and achieves scores comparable to the partially open-source Qwen3 series.

5 Pre-training: Balance of Capabilities

The notion of *reasoning* in large language models (LLMs) remains both complex and contested. While the term is sometimes used to describe a model’s ability to engage in structured, multi-step inference (Wei et al., 2022; Kojima et al., 2022), it has also become a proxy for improved performance on challenging benchmarks (Srivastava et al., 2022). In this work, we adopt a pragmatic stance: we treat gains on reasoning-centric benchmarks as reasonable evidence of enhanced reasoning *behaviors*, while remaining cautious about equating such gains with genuine reasoning ability in the cognitive sense (Bender & Koller, 2020). Concretely, this entails selecting informative datasets that most effectively enhance the target capability (Section 5.1) and optimizing their combination ratios to maximize knowledge acquisition within the fixed token budget (Section 5.2). Figure 4 illustrates the training pipeline with the full procedure in Appendix 3.

5.1 Selecting Informative Datasets for Target Capability

To systematically assess which pre-training distributions most effectively support downstream reasoning behaviors, a naïve approach would be to pre-train separate models on all combinations of candidate datasets, followed by mid-training and post-training, and then measure performance on reasoning benchmarks. However, this strategy is both computationally prohibitive and prone to overfitting to specific benchmarks.

Instead, we design a leave-one-out (LOO) analysis. We train models from scratch on the entire set of pre-selected high-quality datasets, excluding one dataset at a time. We then trace negative log-likelihood

(NLL) on curated *capability-probing datasets* throughout training. Each *capability-probing dataset* can be viewed as defining a token distribution that implicitly induces the necessary preconditions for reasoning to emerge. Importantly, these distributions are heterogeneous: when learned, they contribute unequally to different reasoning-related capabilities, such as *code understanding*, *general knowledge*, and *mathematical problem solving* (Chen et al., 2021; Hendrycks et al., 2021; Cobbe et al., 2021).

5.1.1 Curation of Representative Datasets and Capability-Probing Dataset

Curating the *capability-probing datasets* is critical: it must be representative of the desired capabilities and sufficiently comprehensive to cover each reasoning category. We describe the process of preparing capability datasets as follows.

Hierarchical Rejection Sampling. To derive a compact *capability-probing datasets* for each domain, we employ a hierarchical rejection sampling pipeline that integrates multiple classifier- and model-based filters, as shown in Figure 5. The objective is to construct a small yet representative target dataset for each capability, such that it can serve as a faithful proxy for reasoning performance while dramatically reducing overall volume during evaluation. For each corpus in Table 3, we first apply the FINEWEB-EDU classifier (Penedo et al., 2024) to select samples with high educational value, retaining only those with classifier scores above 4. Next, we incorporate model-based evaluation by scoring each remaining sample using the Ask-LLM paradigm (Sachdeva et al., 2024). The evaluation prompt asks the model to judge whether a sample should be included in a reasoning-probing dataset, framed as a binary classification task (“1” for inclusion, “0” for exclusion). Rather than relying solely on the hard prediction, we record the probability assigned to “1” as a graded measure of the model’s confidence in the example’s reasoning relevance. For all Ask-LLM scoring, we select the top 10% samples within each dataset. This step complements classifier-based quality filtering by directly capturing signals of reasoning relevance, consistent with recent findings that costly, fine-grained quality samplers can outperform simple maximum-coverage approaches in terms of data efficiency (Sachdeva et al., 2024; Pang et al., 2025; Chen & Zhou, 2025). Next, we apply a domain-specific prompt to Ask-LLM for each capability with specific emphasis on code, math, general knowledge or combined. Finally, we perform semantic deduplication across corpora, shrinking each dataset in Table 3 to a subset of roughly 10,000 examples. This yields the **representative datasets** \mathcal{D}^R_i , each containing highly representative samples for its corresponding corpus.

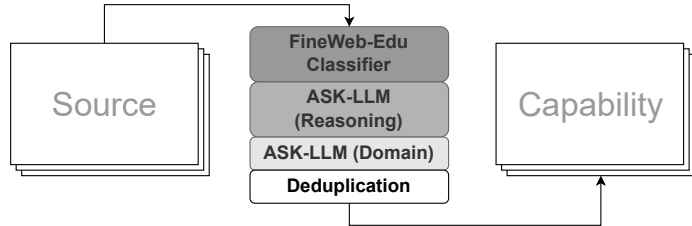


Figure 5 Hierarchical rejection sampling. We employ the FineWeb-Edu classifier in conjunction with the ASK-LLM paradigm to construct a *representative subset* from each pretraining corpus. Samples are assigned selection scores, and inclusion is determined by thresholding these scores.

We categorize them into three domains according to their composition: Code (\mathcal{C}), Math (\mathcal{M}), and Knowledge (\mathcal{K}):

- $\mathcal{C} = \{\text{StarCoder, StackExchange, Nemotron-Code, Cosmopedia, Natural Reasoning, pes2o}\}$
- $\mathcal{M} = \{\text{OpenWebMath, FineMath, Algebraic Stack, Nemotron-Math, Cosmopedia, Natural Reasoning, pes2o}\}$
- $\mathcal{K} = \{\text{FineWeb-Edu, Wikipedia, Arxiv, Cosmopedia, Nemotron-Science, Natural Reasoning, pes2o}\}$

Note that a single dataset may contain data relevant to multiple domains, in which case its representative subset is included in more than one domain. In this way, we construct three filtered, domain-specialized

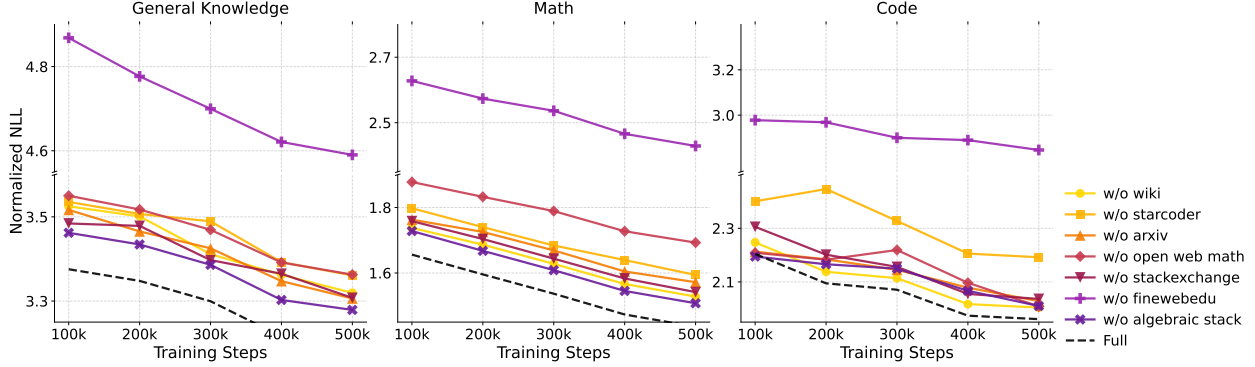


Figure 6 Leave-one-out analysis of pretraining data. The y-axis represents the normalized negative log-likelihood (NLL) on the curated *capability probing datasets*. We systematically exclude individual datasets—StarCoder, OpenWebMath, FineWeb-Edu, Wiki, Arxiv, StackExchange, and Algebraic Stack—to quantify their per-token contributions to downstream performance by comparing them with using full set of data. These trajectories reveal how beneficial each dataset is and how its impact evolves throughout training. Removing FineWeb-Edu yields the largest cross-domain degradation, likely attributable to its broad web-based composition that connects diverse domain.

capability-probing datasets, $\mathcal{D}_{\mathcal{C}, \mathcal{M}, \mathcal{K}}^{\mathcal{P}}$, by combining the representative subsets from all datasets assigned to each domain. We use $(\mathcal{C}, \mathcal{M}, \mathcal{K})$ to denote a **mixture of original datasets** prior to down-sampling.

5.1.2 Disentangling the Impact of Data Sources

We then evaluate the impact of different pretraining corpora on the emergence of reasoning ability by measuring the negative log-likelihood (NLL) on the *capability-probing datasets*. To isolate the contribution of each corpus, we perform rigorous leave-one-out ablation studies, systematically removing individual datasets and measuring the resulting change in NLL across the three *capability-probing datasets* corresponding to *Code*, *Math*, and *General Knowledge* capabilities.

Group Impact via Loss Delta. We define the impact of a dataset \mathcal{D}_j on a reasoning capability as the change in loss it induces on the corresponding *capability-probing dataset* $\mathcal{D}_{\mathcal{C}, \mathcal{M}, \mathcal{K}}^{\mathcal{P}}$. Let $\hat{\theta}$ denote parameters trained on the full dataset $\mathcal{D} = \cup_i \mathcal{D}_i$, and $\hat{\theta}_{-j}$ denote parameters trained with \mathcal{D}_j removed. The *group impact* of \mathcal{D}_j on $\mathcal{D}_c^{\mathcal{P}}, c \in \{\mathcal{C}, \mathcal{M}, \mathcal{K}\}$ is

$$\Delta \mathcal{L}(\mathcal{D}_j, \mathcal{D}_{\mathcal{C}, \mathcal{M}, \mathcal{K}}^{\mathcal{P}}) = \mathbb{E}_{z \sim \mathcal{D}_{\mathcal{C}, \mathcal{M}, \mathcal{K}}^{\mathcal{P}}} [\ell(z; \hat{\theta}_{-j}) - \ell(z; \hat{\theta})], \quad (1)$$

where ℓ is the evaluation loss. A positive value indicates that removing \mathcal{D}_j increases the benchmark loss (i.e., \mathcal{D}_j is beneficial), while a negative value suggests that its presence may hurt performance.

Leave-One-Out Ablations. We operationalize Eq. 1 by training models under leave-one-out settings and measuring the resulting differences in loss across benchmarks. Together, these analyses highlight not only *which* sources matter most, but also *how much* marginal benefit additional data from a given source provides. This methodology allows us to disentangle the contributions of heterogeneous data sources to reasoning-related performance in code, knowledge, and mathematics.

Figure 6 presents the results of our leave-one-out (LOO) experiments across the three evaluated capabilities. To ensure fairness, tokens from each dataset are sampled with equal probability, and no example is repeated during pretraining. Without this normalization, larger datasets such as FINEWEB-EDU would otherwise dominate exposure. We find that excluding FINEWEB-EDU results in the largest degradation across all capabilities, including knowledge, math, and code. We attribute this to its web-based composition, which provides broad and diverse coverage across domains. This result highlights the central role of large-scale web data as a form of “glue” that binds heterogeneous domains together.

In contrast, domain-specific datasets primarily strengthen their respective domains: STARCODER substantially improves code performance (and, interestingly, math), while math-focused corpora primarily benefit math. However, their transfer to general knowledge is limited. An unexpected observation is that STARCODER benefits

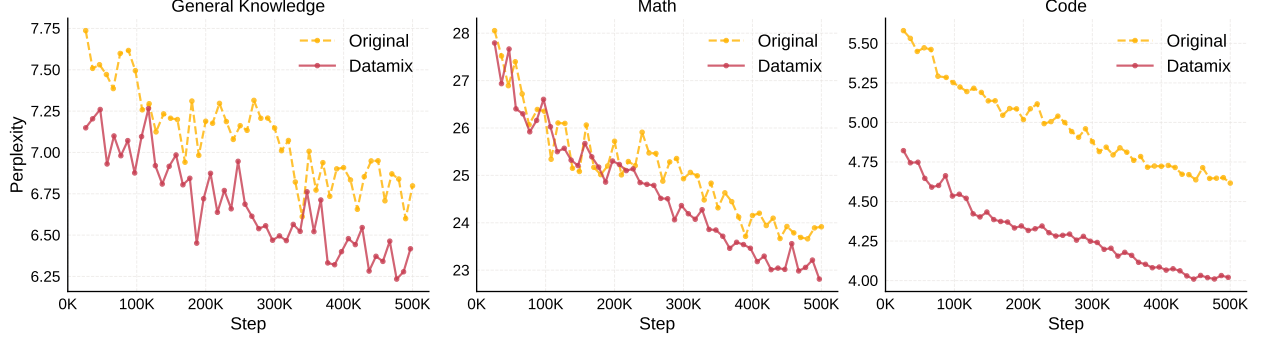


Figure 7 Comparison of data mixture strategies using averaged perplexity. Math is averaged over MATH-500, GSM8K, Code on HumanEval, and General Reasoning is an average of 9 tasks, including ARC-easy, ARC-challenge, BoolQ, PIQA, SIQA, HellaSwag, OBQA, WinoGrand, and MMLU. We compare **Original** (uniform) sampling with our derived **Datamix**. This mixture consistently lowers PPL on Code, Math, and Knowledge benchmarks, despite these benchmarks not being used during training or data selection.

math more than OPENWEB-MATH benefits code, a reversal of the commonly held view that mathematical data contributes disproportionately to coding ability (Lewkowycz et al., 2022). Finally, WIKIPEDIA appears to contribute little to math or code compared to web or domain-specific data, yet remains necessary as a structured and reliable source of factual knowledge.

5.2 Datamixing via Cross-Capability Self-Influence

In Section 5.1.2, we demonstrate that the pre-selected datasets yield measurable utility, as evidenced by reductions in NLL on *capability-probing datasets*. Building on this, we study token budget allocation: given a fixed training budget, how should tokens be distributed across heterogeneous datasets to maximize downstream reasoning performance? Uniform sampling provides a natural baseline but ignores the varying marginal utility of different datasets. Our key insight is that more informative datasets should receive proportionally larger sampling ratios. To operationalize this, we leverage the *influence score* to quantify each dataset’s contribution and guide principled token re-weighting.

Generally, let θ^* denote parameters obtained by training on dataset \mathcal{D} , x_i a training example, x_{test} a example from the target set, which in our case is *capability probing set*, and $\mathcal{L}(x, \theta)$ the loss function. The *influence score* of x_i on the test loss can be approximated as

$$I(x_i, x_{\text{test}}; \theta) = -\nabla_{\theta} \mathcal{L}(x_{\text{test}}; \theta^*)^{\top} H_{\theta^*}^{-1} \nabla_{\theta} \mathcal{L}(x_i; \theta^*), \quad (2)$$

where H_{θ^*} is the Hessian of the training loss at θ^* . While directly computing the Hessian matrix H_{θ^*} is computationally prohibitive for large models, *AutoMixer* (Chang et al., 2025) proposes an efficient approximation method that bypasses explicit Hessian inversion and makes influence score calculation scalable.

We extend the *AutoMixer* framework by treating influence scores as quantitative proxies linking individual training samples to capabilities. Concretely, the influence of a sample on the validation loss of a capability-probing dataset measures the *connection strength* between the sample and the corresponding capability. Rather than using benchmark test sets, we employ samples from *capability-probing datasets* and compute influence scores separately for Code (\mathcal{C}), Math (\mathcal{M}), and Knowledge (\mathcal{K}) domains.

For each training sample x_i from a source dataset, we compute its influence on the validation loss of all three capability-probing datasets. We term this “self-influence” when training and validation samples originate from the same capability and “cross-influence” if they target different capabilities. Because the source datasets are substantially large, we develop an efficient influence estimation algorithm that operates on the *representative dataset* (defined in Section 5.1.1) of each source in Table 3, yielding a computationally scalable surrogate that faithfully preserves cross-capability contribution signals. Concretely, if $x_i \in \mathcal{D}_{\text{StarCoder}}^{\mathcal{R}} \subset \mathcal{D}_{\mathcal{C}}^{\mathcal{P}}$, we evaluate

$$\text{Self-influence: } \mathcal{I}(x_i, x_{\text{test}} \in \mathcal{D}_{\mathcal{C}}^{\mathcal{P}}; \theta_{\mathcal{C}, t}), \quad (3)$$

$$\text{Cross-influence: } \mathcal{I}(x_i, x_{\text{test}} \in \mathcal{D}_{\mathcal{M}}^{\mathcal{P}}; \theta_{\mathcal{M}, t}), \quad \mathcal{I}(x_i, x_{\text{test}} \in \mathcal{D}_{\mathcal{K}}^{\mathcal{P}}; \theta_{\mathcal{K}, t}) \quad (4)$$

Here, checkpoints $\theta_{\mathcal{C},t}$, $\theta_{\mathcal{M},t}$, and $\theta_{\mathcal{K},t}$ are obtained by training separate models to convergence on the full training sets of domains $\mathcal{C}, \mathcal{M}, \mathcal{K}$, yielding domain-specialized parameters. Following the *AutoMixer* protocol, a single checkpoint is insufficient to capture the full training dynamics. We therefore compute influence scores at $T = 10$ evenly spaced checkpoints, weighting each score proportionally to its training step to emphasize later-stage training. These weighted scores quantify the evolving influence of example x_i on the Code, Math, and Knowledge domains throughout training.

Then, the joint influence of a sample is computed as

$$\mathcal{I}_{\text{joint}}(x_i) = \sum_{c \in \{\mathcal{C}, \mathcal{M}, \mathcal{K}\}} \sum_{t=1}^T \alpha_{c,t} \cdot \mathcal{I}(x_i; \theta_{c,t}), \quad (5)$$

where $\theta_{c,t}$ is the checkpoint t for capability c , and $\alpha_{c,t}$ are blending factors reflecting acquisition speed across checkpoints. We assign linearly increasing weights $\alpha_{c,t} \propto t$ across the T checkpoints, and maintain uniform weights across capabilities c .

Each source dataset g is then assigned a sampling weight (w_g):

$$w_g = \frac{\rho_g}{\sum_{g'} \rho_{g'}}, \quad \rho_g = \frac{1}{N_g} \sum_{x_i \in g} \mathcal{I}_{\text{joint}}(x_i) \cdot s_i, \quad (6)$$

with N_g the token count of dataset g and s_i the length of sample x_i . The resulting mixture respects the global budget N while prioritizing datasets whose samples show strong self- and cross-capability connections.

In this setup, we derive a closed-form solution for the data mixture ratio, enabling effective utilization of the limited token budget while enhancing each dataset’s contribution to model performance. Using the *representative datasets* and *capability probing datasets* sampled from the training corpus, it makes influence score computation tractable and exposes how strongly each source dataset (Table 3) contributes to Code, Math, and Knowledge capabilities. This formulation enables principled weighting at the *dataset level*, grounding the mixture in empirically measured cross-domain influences rather than heuristic allocation. As illustrated in Figure 7, the resulting mixture consistently outperforms uniform sampling on Code, Math, and Knowledge benchmarks—none of which are accessed during training or mixture construction—demonstrating the potential for benchmark-free, self-adaptive data optimization.

6 Mid-training: Knowledge Compression

After the model has been exposed to broad knowledge during pretraining, the mid-training phase focuses on compressing this knowledge and maximizing performance on target tasks. We design each mid-training phase with a limited budget of 100B tokens. Unlike pretraining, mid-training induces dramatic shifts in weight distributions and necessitates a more sophisticated, co-evolving model–data mixture strategy. To this end, we propose a novel mid-training paradigm that enables self-boosting: the model trained on a given data mixture is used to compute influence scores for samples, which are then leveraged to dynamically remove negative influence samples and adjust the data sampling ratios for the next phase. As training progresses, the influence scores of data samples increasingly concentrate around zero or negative values, indicating near-complete utilization of the informative content in the dataset and convergence of the process. Notably, this self-evolving scheme requires no access to external benchmark datasets, yet it substantially improves performance on target benchmarks relative to uniform sampling.

We build upon the Dolmino dataset, which has been shown in the OLMo 2 (OLMo et al., 2024) to be an effective mid-training corpus. To enhance domain specialization, we augment Dolmino with additional mathematics and programming data, aiming to strengthen the model’s math and coding capabilities. Given a training example x_i from the mid-training dataset and a probe example x_{test} from *capability probing dataset* $\mathcal{D}_{\mathcal{C}, \mathcal{M}, \mathcal{K}}^P$, we calculate the influence score $\mathcal{I}(x_i, x_{\text{test}}; \theta)$. Here, rather than relying on separately trained models for domain-specific corpora, we leverage the pretrained model θ to capture the dataset requirements at the current stage of training. The data–model co-evolution proceeds iteratively through the following steps:

(1) *Sample-level influence for rejection sampling.* Intuitively, this step acts as a filtering mechanism: only

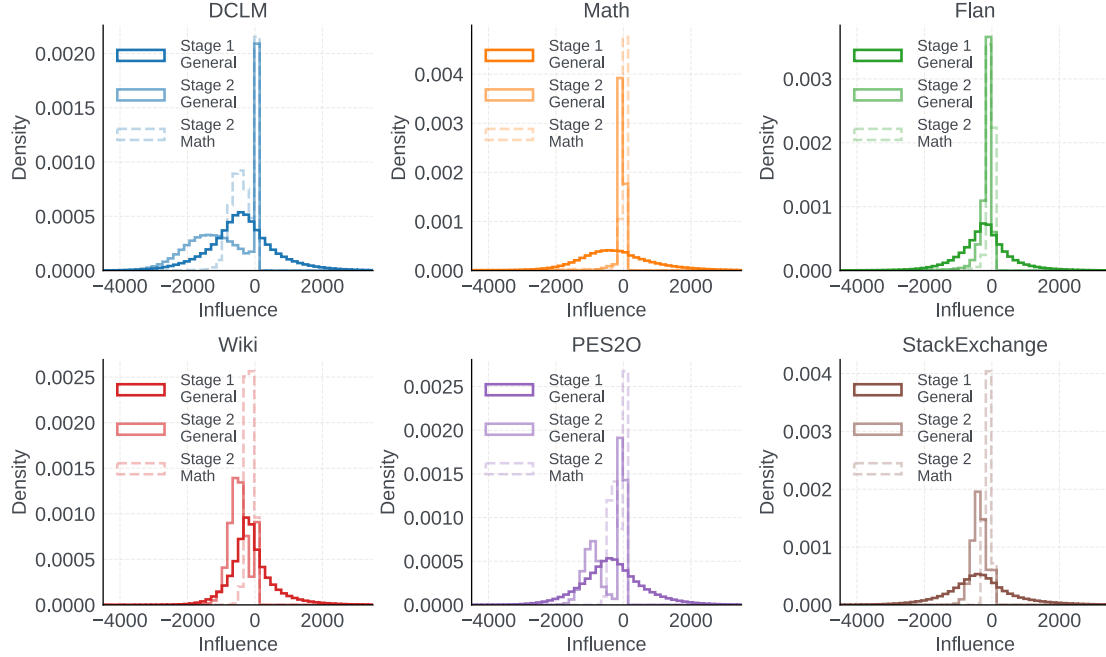


Figure 8 Histogram of influence scores for the general knowledge and math capabilities. In phase 1, data samples exhibit varied influence scores. As training progresses, most samples eventually attain zero or negative influence scores, indicating a convergence point in the model–data co-evolution. At this stage, the dataset’s information has been largely exhausted and can no longer contribute to further model improvement.

training examples that positively contribute to the target capabilities are retained, while neutral or detrimental samples are discarded. Given the raw mid-training dataset $\mathcal{D}^{(\text{raw})}$, at compression phase t we define the retained dataset as:

$$\mathcal{D}_t = \{x_i \in \mathcal{D}^{(\text{raw})} : I(x_i; \theta_t) > 0\}, \quad (7)$$

where θ_t is the model state at phase t . This rejection sampling can be interpreted as an iterative data distillation process: the model continually refines its training distribution, focusing only on samples that yield positive transfer toward the target probing dataset.

(2) *Dataset-level influence for adaptive data mixing.* Beyond sample-level filtering, we aggregate influence scores to the dataset level, enabling adaptive control of the mixing ratio among mid-training datasets, according to Eqs. 5 and 6.

(3) *Train the model on the curated data and repeat the iterative process.* The compressed dataset with the updated mix ratio is used for continued mid-training:

$$\theta_{t+1} = \text{MidTrain}(\theta_t, \mathcal{D}_t). \quad (8)$$

and the updated model θ_{t+1} provides refined influence scores for the next stage. This iterative compression continues until no additional samples yield a positive influence score. In practice, we find that two stages suffice to produce a well-compressed dataset that balances generality with targeted capability improvements.

Intuition: Distributional Compression of Influence. The compression phases can be viewed as iteratively distilling the mid-training dataset in alignment with the model’s evolving capacity throughout training. In early phases, the influence scores are more varied because the model θ_t is still under-trained. However, as t increases, the model becomes better aligned with the target distribution, and its estimates of sample importance are narrowed down (See Figure 8). This recursive interplay produces increasingly refined datasets: uninformative (or negative-influence) samples are discarded, thus amplifying the impact of high-value samples. Conceptually, compression phases mimic an iterative denoising process, where each step sharpens the signal from $\mathcal{D}^{(\text{target})}$ against the noisy background of $\mathcal{D}^{(\text{raw})}$. We terminate the iteration until the distribution of influence converges to approximately zero.

Figure 8 shows histograms of influence scores for general knowledge and math across stage 1 and stage 2 of training. During stage 2, the distribution of influence scores undergoes a pronounced “compression”:

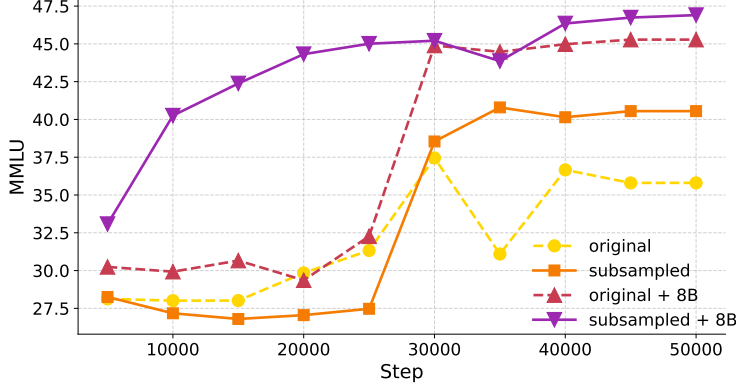


Figure 9 Comparison of the impact on the MMLU benchmark between the original mid-training data and the subsampled data, with and without knowledge distillation.

the range of values narrows, and extreme contributions become less pronounced. Intuitively, as the model becomes more capable, the influence of individual data samples converges toward zero, indicating diminishing impact on downstream reasoning performance. We further highlight the effect of this influence compression in Figure 9. Subsampled mid-training data consistently outperforms the original mid-training set under both standard cross-entropy training and knowledge distillation. Notably, the original data experiences a pronounced performance dip around 30K steps, whereas the subsampled data maintains higher downstream performance throughout training. A similar trend occurs with knowledge distillation using the LLaMa3-8B teacher model, though the performance gap is slightly smaller than under pure cross-entropy. These results indicate that compressing influence scores effectively identifies and preserves the most informative samples, leading to more robust and stable performance trends.

7 Post-Training

Using the datasets from Sections 5 and 6, we obtain MobileLLM-R1-base. Given that our primary goal is to elucidate how data curation in pre-training and mid-training builds strong small reasoning models, we leverage established supervised fine-tuning (SFT) datasets. We first apply Tülu-3-SFT (Lambert et al., 2024) dataset for instruction alignment and OpenScienceReasoning-2, OpenCodeReasoning-2 (Ahmad et al., 2025) and OpenMathReasoning (Moshkov et al., 2025) for reasoning-oriented SFT to extend context and elicit long chain-of-thought reasoning.

7.1 Post-training data

Tülu-3-SFT (Lambert et al., 2024) is a large, curated collection of prompts and instruction-answer pairs designed for post-training language models across skills such as reasoning, coding, and math. It combines publicly available datasets with synthetically generated data. We use tulu-3-sft-olmo-2-mixture-0225, which is a latest filtered version of Tulu-3 dataset.

OpenMathReasoning (Moshkov et al., 2025) is a large-scale dataset for training models in complex mathematical reasoning. It contains 3.2M long chain-of-thought (CoT) solutions for 306K unique mathematical problems, helping models improve problem-solving skills in mathematics.

OpenScienceReasoning-2 (NVIDIA, 2025) is a synthetic dataset spanning multiple scientific domains. It contains 803k general-purpose reasoning data, including STEM, law, economics, and humanities, featuring both multiple-choice and open-ended questions, designed to enhance scientific reasoning capabilities.

OpenCodeReasoning-2 (Ahmad et al., 2025) is a large-scale dataset for programming reasoning. It contains 1.4M Python and 1.1M C++ samples, covering nearly 35K unique competitive programming problems. It is intended to improve code completion abilities in models.

7.2 Post-training ablation

We conduct ablation studies to understand the contribution of different supervision signals and training strategies in our two-stage post-training pipeline. Results in Table 8 reflect several interesting insights.

(1) *Instruction-following supervision provides a strong foundation for reasoning.* Models that are first trained with Tulu-SFT data consistently outperform those that start directly from reasoning data. This demonstrates that high-quality instruction-following supervision provides alignment signals making subsequent reasoning adaptation more effective.

(2) *Domain-specific data improves performance in its own domain.* OpenMathReasoning, OpenScienceReasoning-2, and OpenCodeReasoning-2 improve performance on math, code, and knowledge-intensive benchmarks (e.g., MMLU), respectively. These effects are highly consistent, showing that specialized datasets provide targeted benefits.

(3) *Scientific reasoning data generalizes across domains.* Beyond its impact on MMLU, adding science data also improves performance on math and coding tasks compared to using only math and coding data. This suggests that scientific reasoning provides broadly useful structures that transfer across different forms of symbolic problem-solving.

(4) *Symbolic Reasoning Gains Come at the Cost of Knowledge Retention.* Introducing math or coding data tends to reduce performance on MMLU. We hypothesize this is due to limited model capacity: when the model is pushed to absorb new symbolic reasoning skills through exposure to math and coding data, it partially forgets factual knowledge that is important for knowledge-intensive evaluation. This forgetting effect

Table 8 Ablation studies on post-training stages. We use M, S, C to denote OpenMathReasoning, OpenScienceReasoning-2 and OpenCodeReasoning-2 datasets respectively.

Stage 1	Stage 2	MATH	GSM8K	LCBv6	MMLU
<i>Ablation on Stage 1</i>					
w/o Tulu-3	M + C + S	56.2	68.2	13.1	44.0
w/ Tulu-3	M + C + S	57.8	68.5	13.7	43.7
<i>Ablation on Stage 2</i>					
Tulu-3	M	57.4	68.2	0.0	43.1
Tulu-3	C	16.2	31.0	12.0	39.9
Tulu-3	S	23.8	62.2	3.4	45.6
Tulu-3	M + C	58.4	65.6	10.9	40.4
Tulu-3	M + S	60.0	66.9	0.6	45.0
Tulu-3	C + S	29.4	65.3	14.3	44.4
Tulu-3	M + C + S	57.8	68.5	13.7	43.7
<i>Joint Ablation</i>					
Tulu-3 + (M + C + S)	–	56.2	53.1	14.9	44.0
Tulu-3	(M + C + S)	57.8	68.5	13.7	44.0

Table 9 Evaluation of reasoning capabilities elicited by different models when fine-tuned on the same reasoning supervised finetuning (SFT) dataset. Baseline models use their instruct checkpoints; OLMo uses its SFT checkpoint before reinforcement learning; our model uses intermediate Tulu3-SFT checkpoints, denoted with *. All models are trained for one epoch on the joint reasoning SFT corpus (OpenMathReasoning + OpenScienceReasoning-2 + OpenCodeReasoning-2).

Model	Size	MATH	GSM8K	LCBv6
SmolLM2-135M-Instruct	135M	3.2	1.6	0.6
MobileLLM-R1-140M*	140M	4.8	3.7	1.1
SmolLM2-360M-Instruct	362M	5.2	7.4	3.4
MobileLLM-R1-360M*	359M	19.2	23.8	4.0
OLMo-2-0425-1B-SFT	1.48B	53.0	58.8	11.4
SmolLM2-1.7B-Instruct	1.71B	41.4	50.5	7.4
MobileLLM-R1-950M*	949M	57.8	68.5	13.7

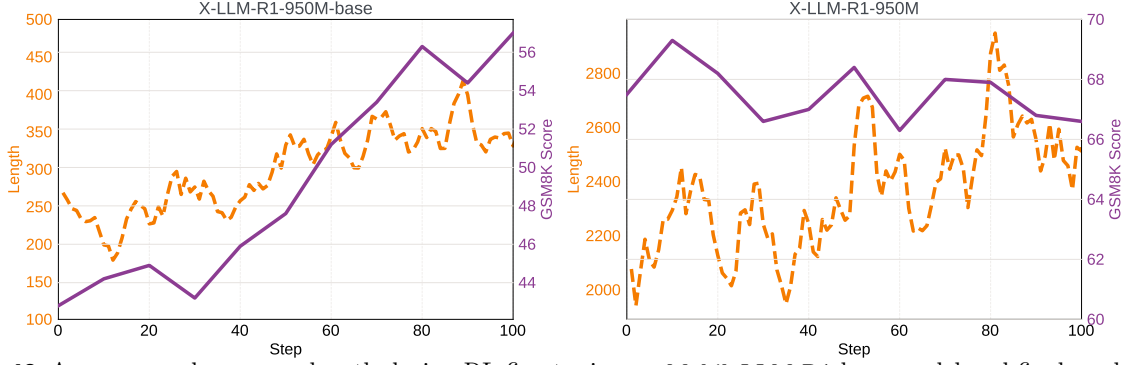


Figure 10 Accuracy and sequence length during RL fine-tuning on MobileLLM-R1 base model and final model after supervised finetuning (SFT). Small models benefit from RL when pretrained on a suitable corpus, with MobileLLM-R1-950M-base showing steady reasoning gains. However, small model trained with SFT data outperforms base+RL, and additional RL can degrade small models optimized with SFT.

is especially pronounced in smaller models.

(5) *Decoupling Alignment and Reasoning for Stronger Models.* Compared to Model trained with Tulu and reasoning data jointly in a single stage, a two-stage setup of first training on Tulu, then on reasoning data delivers overall stronger results especially on math and general reasoning benchmarks.

7.3 Comparison with baselines on identical reasoning SFT

To disentangle the contribution of curated pre-training and mid-training data from that of high-quality post-training data, we conducted an ablation study. Specifically, we finetune all baseline instruct models, as well as the MobileLLM-R1 general supervised fine-tuned model (trained for 2 epochs on the Tulu dataset), on the joint reasoning SFT corpus (OpenMathReasoning + OpenScienceReasoning-2 + OpenCodeReasoning-2) for one epoch. Our results in Table 9 show that, even under identical supervised fine-tuning, models with stronger pre-training and mid-training exhibit more robustly embedded knowledge, which in turn facilitates the elicitation of reasoning capabilities during post-training. In that sense, MobileLLM-R1 consistently outperforms prior models trained on fully open-source corpora, such as OLMo-2 and SmoLLM, on reasoning benchmarks. Notably, our 140M and 360M checkpoints achieve substantial gains over SmoLLM baselines, while our 950M model surpasses both OLMo-2 1.48B and SmoLLM-1.7B, despite its significantly smaller size.

7.4 Discussion: Whether to Use RL or Not

A central question in the development of small reasoning language models is whether reinforcement learning (RL) is beneficial. Recent works such as DeepSeek-R1 (Guo et al., 2025) and Qwen3 (Yang et al., 2025) adopt a two-stage paradigm: (i) train a large model with RL, and (ii) generate strong reasoning traces to distill smaller student models, either via sequence-level distillation or a combination of logit-level and sequence-level distillation. The underlying rationale is that large models, equipped with greater exploration capacity and self-improvement potential, can discover more effective reasoning trajectories, while small models, being capacity-constrained, are better suited to imitating curated demonstrations rather than performing exploration directly.

To assess the impact of reinforcement learning (RL) on small reasoning models, we perform an ablation study by applying an RL stage to both the base model and the final model, i.e., fine-tuned with SFT data. The base model is finetuned for 100 steps on the TULU3 dataset (1% of total data) as a cold start, solely to learn the correct output format. Subsequently, both the base and SFT models undergo GRPO training on the NuminaMath-TIR dataset with a learning rate of 3×10^{-6} , 100 training steps, a batch size of 32 prompts, and 8 generations per prompt. The KL coefficient for the reference model is set to $\beta = 0$.

The results in Figure 10 highlight several key observations: (1) Small models can also benefit from RL-based fine-tuning when they are well-pretrained on a suitable corpus. Results show that MobileLLM-R1-950M-base achieves evident improvements in reasoning accuracy as the average length gradually increases. (2) Supervised fine-tuning (SFT) data distilled from large models, with data source listed in Table 5, consistently yields higher

Table 10 Generation speed (token/s) across context lengths for different model sizes. OOM indicates out-of-memory.

Model	Size	1k	2k	4k	8k	16k	32k
MobileLLM-R1-140M	140M	129.67	116.16	111.42	110.47	96.38	79.71
MobileLLM-R1-350M	360M	77.23	61.54	61.24	61.27	61.13	OOM
MobileLLM-R1-900M	950M	31.05	27.59	25.09	25.36	OOM	OOM
LLaMA3.2-1B	1.24B	28.71	24.99	21.99	22.00	OOM	OOM
LLaMA3.2-3B	3.21B	9.04	8.61	OOM	OOM	OOM	OOM
LLaMA3.1-8B	8.03B	2.76	OOM	OOM	OOM	OOM	OOM

performance than directly applying RL to small models, corroborating prior findings. For instance, the final GSM8K accuracy of RL-optimized MobileLLM-R1-950M-base is 57.0, compared to 74.0 for the SFT-trained MobileLLM-R1-950M. (3) For high-performing small models fully fine-tuned on SFT data, additional RL does not observe a significant performance improvement. This suggests that SFT provides more structured and reliable supervision than the noisy self-exploration signal accessible to small models, which often lack the capacity to further refine their reasoning policies beyond the distilled demonstrations.

8 On-device Profiling

Table 10 reports the measured generation throughput (tokens per second) of MobileLLM-R1 models and LLaMA-3 baselines across different context lengths on the Samsung Galaxy S22. The results confirm the clear efficiency advantage of smaller models: the 140M variant sustains over 100 tokens/s up to 8k tokens, while even the 360M and 950M models maintain practical throughput across medium-length contexts. In contrast, larger models such as LLaMA-3.2-3B and LLaMA-3.1-8B encounter out-of-memory failures beyond short contexts, and the LLaMA-3.2-1B model runs at less than one-quarter the speed of MobileLLM-R1-140M. Moreover, long-context settings (16k–32k) quickly exhaust memory capacity for billion-scale models, highlighting the prohibitive cost of KV-cache storage at scale. These findings demonstrate that sub-billion parameter models not only enable reasoning with reduced memory overhead but also achieve far higher generation speed, making them far better suited for on-device long-context inference. We benchmark the latency of MobileLLM-R1 models (140M, 360M, 950M) and LLaMA-3 models (1B, 3B, 8B) using ExecuTorch on a Samsung Galaxy S22 (8 GB RAM). In this experiment, we run each model with a warm-up phase and then average the results over three iterations using the same prompt. On-device applications usually adopt quantized settings. To reflect typical on-device deployment, models are benchmarked under quantized settings: linear layers are quantized using 8-bit dynamic activations and 4-bit weights. For the 125M model, a group size of 32 is adopted since its hidden dimension is not divisible by 128, whereas all larger models use a group size of 128. Embedding layers are quantized to 4-bit with a group size of 32.

Latency is reported in tokens per second across generation lengths ranging from 1k to 32k. As expected, latency decreases as context length grows and as model size increases. When context length becomes large, the KV cache size approaches the size of the weights. Since we are already memory-bound when loading weights, the additional cost of loading the KV cache is no longer negligible.

For long-context reasoning, the sequence length can rapidly extend to 32k tokens. At this scale, larger models quickly hit memory constraints. Thus, enabling efficient long-context on-device reasoning necessitates smaller models. Beyond memory efficiency, smaller models also provide significantly higher generation throughput, as speed scales approximately inversely with model size, underscoring the importance of compact models for practical on-device reasoning.

9 Related Work

The advent of GPT-3 (Brown et al., 2020) demonstrated the transformative potential of large language models (LLMs), catalyzing a wave of research on LLMs, including both proprietary models like Claude (Anthropic, 2024), and open-source alternatives such as LLaMA (Touvron et al., 2023a,b; Dubey et al., 2024), Gemma (Team et al., 2024a,b, 2025), Qwen (Team, 2024; Yang et al., 2025), etc. The scaling laws of large language models (LLMs) have long been a central focus in the field. Researchers are particularly interested in understanding

how increasing model size can elicit emergent capabilities and whether there exist potential singularities in performance. Concurrently, there is growing attention on the efficiency-accuracy trade-offs achievable with smaller models. Investigating the performance limits of parameter-constrained models not only elucidates the fundamental boundaries of representational capacity but also highlights opportunities for optimizing computational efficiency and resource utilization. Notably, MobileLLM (Liu et al., 2024) represents the first LLM explicitly designed for on-device deployment. Subsequently, numerous high-performance and small-scale models, including OLMO (OLMo et al., 2024), SmoLLM (Allal et al., 2025) have been open-sourced. Moreover, these work also denotes a broader trend toward transparency in model development. Beside opensourcing the model weights, they also have provided both weights, training data sources and full training pipelines.

Recently, research focus has gradually shifted from System I to System II thinking, i.e., from instinctive outputs to eliciting explicit reasoning capabilities through methods since the introduction of OpenAI’s O1 model (Jaech et al., 2024). The release of DeepSeek-R1 marked a very successful instance of exposing a model training process explicitly aimed at enhancing reasoning (Guo et al., 2025). Qwen (Yang et al., 2025) represents another strong example of building high-quality reasoning models, with its smaller-scale variants consistently achieving state-of-the-art results across benchmark evaluations.

Prior studies have consistently shown that reasoning capabilities typically emerge only after training on extremely large corpora of tokens (Yang et al., 2025). In contrast, our work shows that a small model can achieve strong reasoning abilities without massive datasets. Table 11 compares state-of-the-art open-source language models under the sub-billion parameter regime, highlighting differences in training scale, context length, openness, and reasoning support. Most prior approaches rely on in-context CoT prompting to elicit reasoning, whereas MobileLLM-R1 and Qwen3 explicitly optimize on long-form reasoning traces, enabling the generation of multi-step reasoning sequences without dependence on prompt-based process. While many recent models, such as Qwen 3 (0.6B, 36T tokens) and LLaMA 3.2 (1.24B, 9T tokens), rely on extremely large proprietary or partially open datasets, only a few—including SmoLLM2, OLMO 2, and our proposed MobileLLM-R1 series—provide both weights and fully reproducible training recipes. Notably, despite using significantly fewer training tokens (4.2T) than models like Qwen 3, MobileLLM-R1 achieves competitive or superior reasoning capabilities, underscoring the importance of dataset curation over sheer scale.

Table 11 Comparison of attributes of state-of-the-art sub-billion parameter (< 1B or \approx 1B) language models

Name	Sizes (# Params)	# Training tokens	Context length	OSS weights	OSS data source & full recipe	Model type
SmoLLM2	135M, 360M	2T (135M), 4T (360M)	8k	✓	✓	Instruct
OLMO 2	1B (1.48B)	4.5T	4k	✓	✓	Instruct
Qwen 2.5	0.5B	18T	32k	✓	✗	Instruct
Qwen 3	0.6B	36T	32k	✓	✗	Thinking
LLaMA 3.2	1B (1.24B)	9T	128k	✓	✗	Instruct
Gemma 3	270M, 1B	6T (270M), 2T (1B)	32k	✓	✗	Instruct
MobileLLM	125M, 350M, 600M, 1B	1T	2k	✓	✗	Base
MobileLLM-R1	140M, 360M, 950M	4.2T	32k	✓	✓	Thinking

10 Conclusion

We present a data-centric framework to maximize reasoning in small language models under limited parameters and tokens. We introduce benchmark-free, self-evolving data optimization, a principled dataset-level weighting method that leverages cross-domain influences to dynamically tailor the data mixture. This approach enables strong performance on code, math, and knowledge benchmarks without exposing any benchmark data during training or mixture construction. Trained on 4.2T tokens drawn from \sim 2T curated open-source data, MobileLLM-R1 achieves state-of-the-art results among small models with a fully open-sourced recipe, and matches Qwen3-0.6B with only 11.7% of its 36T-token training data. Our findings challenge the conventional belief that small reasoning models require massive data, instead underscoring the pivotal role of data quality, token efficiency, and principled data curation.

References

- Josh Achiam, Steven Adler, Sandhini Agarwal, Lama Ahmad, Ilge Akkaya, Florencia Leoni Aleman, Diogo Almeida, Janko Altenschmidt, Sam Altman, Shyamal Anadkat, et al. Gpt-4 technical report. *arXiv preprint arXiv:2303.08774*, 2023.
- Wasi Uddin Ahmad, Somshubra Majumdar, Aleksander Ficek, Sean Narenthiran, Mehrzad Samadi, Jocelyn Huang, Siddhartha Jain, Vahid Noroozi, and Boris Ginsburg. Opencodereasoning-ii: A simple test time scaling approach via self-critique. *arXiv preprint arXiv:2507.09075*, 2025.
- Loubna Ben Allal, Anton Lozhkov, Elie Bakouch, Gabriel Martín Blázquez, Guilherme Penedo, Lewis Tunstall, Andrés Marafioti, Hynek Kydlíček, Agustín Piqueres Lajarín, Vaibhav Srivastav, et al. Smollm2: When smol goes big-data-centric training of a small language model. *arXiv preprint arXiv:2502.02737*, 2025.
- Anthropic. Claude. <https://claude.ai>, 2024. Large language model.
- Emily M. Bender and Alexander Koller. Climbing towards NLP’s Everest: Avoiding the pitfall of understanding. In *Proceedings of the 58th Annual Meeting of the Association for Computational Linguistics*, pp. 5185–5198, 2020.
- Tom Brown, Benjamin Mann, Nick Ryder, Melanie Subbiah, Jared D Kaplan, Prafulla Dhariwal, Arvind Neelakantan, Pranav Shyam, Girish Sastry, Amanda Askell, et al. Language models are few-shot learners. *Advances in neural information processing systems*, 33:1877–1901, 2020.
- Ernie Chang, Yang Li, Patrick Huber, Vish Vogeti, David Kant, Yangyang Shi, and Vikas Chandra. AutoMixer: Checkpoint artifacts as automatic data mixers. In Wanxiang Che, Joyce Nabende, Ekaterina Shutova, and Mohammad Taher Pilehvar (eds.), *Proceedings of the 63rd Annual Meeting of the Association for Computational Linguistics (Volume 1: Long Papers)*, pp. 19942–19953, Vienna, Austria, July 2025. Association for Computational Linguistics. ISBN 979-8-89176-251-0. doi: 10.18653/v1/2025.acl-long.979. URL <https://aclanthology.org/2025.acl-long.979>.
- Fei Chen and WENCHI Zhou. Quality over quantity: An effective large-scale data reduction strategy based on pointwise v-information. *arXiv preprint arXiv:2507.00038*, 2025. URL <https://arxiv.org/abs/2507.00038>.
- Mark Chen, Jerry Tworek, Heewoo Jun, Qiming Yuan, et al. Evaluating large language models trained on code. In *arXiv preprint arXiv:2107.03374*, 2021.
- Karl Cobbe, Vineet Kosaraju, Mohammad Bavarian, Mark Chen, et al. Training verifiers to solve math word problems. In *arXiv preprint arXiv:2110.14168*, 2021.
- Abhimanyu Dubey, Abhinav Jauhri, Abhinav Pandey, Abhishek Kadian, Ahmad Al-Dahle, Aiesha Letman, Akhil Mathur, Alan Schelten, Amy Yang, Angela Fan, et al. The llama 3 herd of models. *arXiv e-prints*, pp. arXiv–2407, 2024.
- Nelson Elhage, Tristan Hume, Catherine Olsson, Nicholas Schiefer, Tom Henighan, Shauna Kravec, Zac Hatfield-Dodds, Robert Lasenby, Dawn Drain, Carol Chen, et al. Toy models of superposition. *arXiv preprint arXiv:2209.10652*, 2022.
- Quentin Garrido, Randall Balestrieri, Laurent Najman, and Yann Lecun. Rankme: Assessing the downstream performance of pretrained self-supervised representations by their rank. In *International conference on machine learning*, pp. 10929–10974. PMLR, 2023.
- Daya Guo, Dejian Yang, Haowei Zhang, Junxiao Song, Ruoyu Zhang, Runxin Xu, Qihao Zhu, Shirong Ma, Peiyi Wang, Xiao Bi, et al. Deepseek-r1: Incentivizing reasoning capability in llms via reinforcement learning. *arXiv preprint arXiv:2501.12948*, 2025.
- Dan Hendrycks, Collin Burns, Steven Basart, Andy Zou, Mantas Mazeika, Dawn Song, and Jacob Steinhardt. Measuring massive multitask language understanding. In *International Conference on Learning Representations (ICLR)*, 2021.
- Aaron Jaech, Adam Kalai, Adam Lerer, Adam Richardson, Ahmed El-Kishky, Aiden Low, Alec Helyar, Aleksander Madry, Alex Beutel, Alex Carney, et al. Openai o1 system card. *arXiv preprint arXiv:2412.16720*, 2024.
- Takeshi Kojima, Shixiang Shane Gu, Machel Reid, Yutaka Matsuo, and Yusuke Iwasawa. Large language models are zero-shot reasoners. In *Advances in Neural Information Processing Systems (NeurIPS)*, 2022.
- Nathan Lambert, Jacob Morrison, Valentina Pyatkin, Shengyi Huang, Hamish Ivison, Faeze Brahman, Lester James V. Miranda, Alisa Liu, Nouha Dziri, Shane Lyu, Yuling Gu, Saumya Malik, Victoria Graf, Jena D. Hwang, Jiangjiang

Yang, Ronan Le Bras, Oyvind Tafjord, Chris Wilhelm, Luca Soldaini, Noah A. Smith, Yizhong Wang, Pradeep Dasigi, and Hannaneh Hajishirzi. Tülu 3: Pushing frontiers in open language model post-training. 2024.

Aitor Lewkowycz, Anders Johan Andreassen, David Dohan, Ethan Dyer, Henryk Michalewski, Vinay Venkatesh Ramasesh, Ambrose Sloane, Cem Anil, Imanol Schlag, Theo Gutman-Solo, Yuhuai Wu, Behnam Neyshabur, Guy Gur-Ari, and Vedant Misra. Solving quantitative reasoning problems with language models. *arXiv preprint arXiv:2206.14858*, 2022. URL <https://arxiv.org/abs/2206.14858>.

Dacheng Li, Shiyi Cao, Tyler Griggs, Shu Liu, Xiangxi Mo, Eric Tang, Sumanth Hegde, Kourosh Hakhamaneshi, Shishir G Patil, Matei Zaharia, et al. Llms can easily learn to reason from demonstrations structure, not content, is what matters! *arXiv preprint arXiv:2502.07374*, 2025.

Zechun Liu, Changsheng Zhao, Forrest Iandola, Chen Lai, Yuandong Tian, Igor Fedorov, Yunyang Xiong, Ernie Chang, Yangyang Shi, Raghuraman Krishnamoorthi, et al. Mobilellm: Optimizing sub-billion parameter language models for on-device use cases. In *Forty-first International Conference on Machine Learning*, 2024.

Ivan Moshkov, Darragh Hanley, Ivan Sorokin, Shubham Toshniwal, Christof Henkel, Benedikt Schifferer, Wei Du, and Igor Gitman. Aimo-2 winning solution: Building state-of-the-art mathematical reasoning models with openmathreasoning dataset. *arXiv preprint arXiv:2504.16891*, 2025.

NVIDIA. Opensciencereasoning-2 dataset, 2025. URL <https://huggingface.co/datasets/nvidia/OpenScienceReasoning-2>.

Team OLMo, Pete Walsh, Luca Soldaini, Dirk Groeneveld, Kyle Lo, Shane Arora, Akshita Bhagia, Yuling Gu, Shengyi Huang, Matt Jordan, et al. 2 olmo 2 furious. *arXiv preprint arXiv:2501.00656*, 2024.

Xi Pang et al. Fine-grained data selection for llm supervised fine-tuning. *arXiv preprint arXiv:2502.01968*, 2025. URL <https://arxiv.org/abs/2502.01968>.

Guilherme Penedo, Hynek Kydlíček, Anton Lozhkov, Margaret Mitchell, Colin A Raffel, Leandro Von Werra, Thomas Wolf, et al. The fineweb datasets: Decanting the web for the finest text data at scale. *Advances in Neural Information Processing Systems*, 37:30811–30849, 2024.

Noveen Sachdeva, Benjamin Coleman, Wang-Cheng Kang, Jianmo Ni, Lichan Hong, Ed H Chi, James Caverlee, Julian McAuley, and Derek Zhiyuan Cheng. How to train data-efficient llms. *arXiv preprint arXiv:2402.09668*, 2024.

Ranajoy Sadhukhan, Zhuoming Chen, Haizhong Zheng, Yang Zhou, Emma Strubell, and Beidi Chen. Kinetics: Rethinking test-time scaling laws. *arXiv preprint arXiv:2506.05333*, 2025.

Aarohi Srivastava et al. Beyond the imitation game: Quantifying and extrapolating the capabilities of language models. In *arXiv preprint arXiv:2206.04615*, 2022.

Gemma Team, Thomas Mesnard, Cassidy Hardin, Robert Dadashi, Surya Bhupatiraju, Shreya Pathak, Laurent Sifre, Morgane Rivière, Mihir Sanjay Kale, Juliette Love, et al. Gemma: Open models based on gemini research and technology. *arXiv preprint arXiv:2403.08295*, 2024a.

Gemma Team, Morgane Rivière, Shreya Pathak, Pier Giuseppe Sessa, Cassidy Hardin, Surya Bhupatiraju, Léonard Hussenot, Thomas Mesnard, Bobak Shahriari, Alexandre Ramé, et al. Gemma 2: Improving open language models at a practical size. *arXiv preprint arXiv:2408.00118*, 2024b.

Gemma Team, Aishwarya Kamath, Johan Ferret, Shreya Pathak, Nino Vieillard, Ramona Merhej, Sarah Perrin, Tatiana Matejovicova, Alexandre Ramé, Morgane Rivière, et al. Gemma 3 technical report. *arXiv preprint arXiv:2503.19786*, 2025.

Qwen Team. Qwen2 technical report. *arXiv preprint arXiv:2407.10671*, 2024.

Hugo Touvron, Thibaut Lavril, Gautier Izacard, Xavier Martinet, Marie-Anne Lachaux, Timothée Lacroix, Baptiste Rozière, Naman Goyal, Eric Hambro, Faisal Azhar, et al. Llama: Open and efficient foundation language models. *arXiv preprint arXiv:2302.13971*, 2023a.

Hugo Touvron, Louis Martin, Kevin Stone, Peter Albert, Amjad Almahairi, Yasmine Babaei, Nikolay Bashlykov, Soumya Batra, Prajjwal Bhargava, Shruti Bhosale, et al. Llama 2: Open foundation and fine-tuned chat models. *arXiv preprint arXiv:2307.09288*, 2023b.

Zengzhi Wang, Fan Zhou, Xuefeng Li, and Pengfei Liu. Octothinker: Mid-training incentivizes reinforcement learning scaling. *arXiv preprint arXiv:2506.20512*, 2025.

Jason Wei, Xuezhi Wang, Dale Schuurmans, Maarten Bosma, Ed H. Chi, Quoc V. Le, and Denny Zhou. Chain-of-thought prompting elicits reasoning in large language models. In *Advances in Neural Information Processing Systems (NeurIPS)*, 2022.

An Yang, Beichen Zhang, Binyuan Hui, Bofei Gao, Bowen Yu, Chengpeng Li, Dayiheng Liu, Jianhong Tu, Jingren Zhou, Junyang Lin, et al. Qwen2. 5-math technical report: Toward mathematical expert model via self-improvement. *arXiv preprint arXiv:2409.12122*, 2024.

An Yang, Anfeng Li, Baosong Yang, Beichen Zhang, Binyuan Hui, Bo Zheng, Bowen Yu, Chang Gao, Chengen Huang, Chenxu Lv, et al. Qwen3 technical report. *arXiv preprint arXiv:2505.09388*, 2025.

Hanlin Zhu, Shibo Hao, Zhiting Hu, Jiantao Jiao, Stuart Russell, and Yuandong Tian. Reasoning by superposition: A theoretical perspective on chain of continuous thought. *arXiv preprint arXiv:2505.12514*, 2025.

Appendix

A Trajectory of Reasoning Capability Across Training Phases

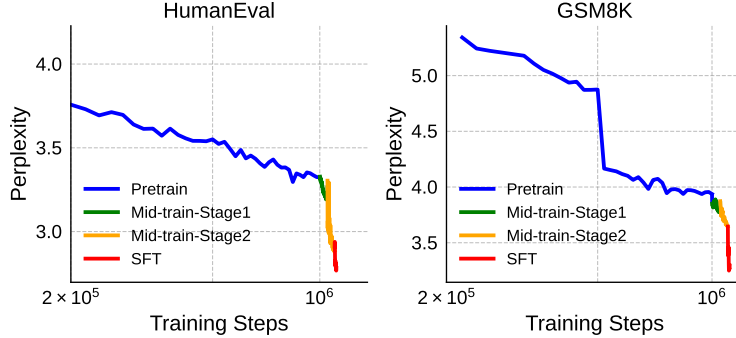


Figure 11 Evolution of reasoning capability during training, measured by perplexity reductions on reasoning-focused benchmarks: HumanEval for coding and GSM8K for math.

While the model undergoes the pre-training, mid-training, and post-training stages, we track its reasoning ability by measuring perplexity on two reasoning-focused benchmarks: HumanEval and GSM8K. Our results in Figure 11 show that the perplexity on math sees a significant drop early during the second phase of pre-training. Interestingly, the same model, when subjected to the second phase of mid-training with limited data, exhibits a dramatic perplexity decrease in HumanEval. This suggests that the knowledge acquired from math training is transferable to coding, enabling the model to develop coding abilities subsequently.

B Learning Rate Affects Representation Learning

We conduct an ablation study on the effect of learning rate during pretraining. The setup employs 16 nodes with 8 GPUs each, a per-device batch size of 8, and training for 500k steps with a sequence length of 2048, corresponding to approximately 1T tokens. The learning rate follows a linear decay schedule from its peak value to 10% of the maximum, with an initial warmup phase of 2k steps. The mid-training stage follows the same optimization recipe as used in our final configuration.

Our results indicate that, while pretraining MMLU performance remains largely unchanged across learning rates, the differences become significant after mid-training, as shown in Table 12. Models pretrained with larger learning rates exhibit superior downstream accuracy, suggesting that they acquire stronger intermediate representations during pretraining. Importantly, pretraining accuracy itself does not provide predictive power for downstream outcomes.

Therefore, we investigate structural diagnostics of pretrained representations that can act as low-cost proxies for downstream generalization. We draw inspiration from RankMe (Garrido et al., 2023), originally proposed in the context of vision self-supervised finetuning:

$$\text{RankMe}(Z) = \exp \left(- \sum_{k=1}^{\min(N, K)} p_k \log p_k \right), \quad \text{where } p_k = \frac{\sigma_k(Z)}{\sum_{i=1}^{\min(N, K)} \sigma_i(Z)} + \epsilon, \quad (9)$$

where $\sigma_k(Z)$ denotes the singular values of output embeddings Z . Our analysis indicates that downstream performance is closely tied to parameter utilization during pretraining: models that activate broader, task-relevant subspaces and maintain high-rank embeddings facilitate fine-tuning to more effectively recover and exploit useful representations.

Table 12 Performance comparison between pre-training and after mid-training under different learning rates.

Learning Rate	Pre-training		After Mid-training	
	MMLU	RankMe Score	MMLU	
4e-3	27.92	21.98	36.31	
2e-3	27.67	20.19	33.95	
1e-3	26.87	14.22	29.02	
4e-4	27.50	7.81	27.55	

In our case, the RankMe score correlates strongly with post mid-training MMLU accuracy, supporting its utility as a proxy measure that could potentially provide early signals and save resources. Furthermore, analysis of the RankMe score shows that higher learning rates lead to higher representational rank. This implies that a larger fraction of parameters are effectively utilized during pretraining, which in turn enables stronger generalization and improved final task accuracy. We note that this is a preliminary study and represents a promising direction for future investigation.

C Per-task Accuracy on Common-Sense Reasoning Benchmarks

Table 13 Per-task accuracies on eight zero-shot common-sense reasoning tasks.

Model	Size	ARC-easy	ARC-challenge	BoolQ	PIQA	SIQA	HellaSwag	OBQA	Winogrande	Avg.
<i><150M</i>										
SmolLM2-135M	135M	58.9	34.5	60.5	68.9	43.5	43.6	41.1	52.8	50.5
MobileLLM-R1-140M-base	140M	47.3	32.5	57.2	62.5	42.6	32.9	31.5	51.0	44.7
<i>150M – 400M</i>										
Gemma-3-270M-pt	268M	57.7	31.5	56.5	68.5	43.1	41.4	34.6	53.9	48.4
SmolLM2-360M	362M	67.9	42.0	63.4	72.1	44.7	56.2	47.4	59.0	56.6
MobileLLM-R1-360M-base	359M	59.8	36.0	65.9	68.3	45.0	42.7	34.4	53.5	50.7
<i>400M – 1B</i>										
Qwen2.5-0.5B	494M	63.3	36.1	56.9	69.4	44.6	50.7	40.7	56.1	52.2
Qwen3-0.6B-Base	596M	66.2	40.3	69.4	69.7	45.5	52.9	40.7	57.9	55.3
MobileLLM-R1-950M-base	949M	66.3	45.3	79.6	74.2	48.4	57.2	39.8	58.2	58.6
<i>>1B</i>										
Gemma-3-1B-pt	1.00B	71.6	37.7	66.3	74.8	45.4	61.9	41.9	58.3	57.2
LLaMA3-2.1B	1.24B	64.8	42.9	64.7	74.9	44.8	64.4	50.0	60.4	58.4
OLMo-2-0425-1B	1.48B	72.2	44.0	68.8	74.5	48.4	66.0	46.0	63.4	60.4
Qwen2.5-1.5B	1.54B	70.4	41.2	73.9	72.9	48.2	65.2	36.3	61.2	58.7
SmolLM2-1.7B	1.71B	73.6	49.5	72.0	77.6	46.1	70.7	47.8	64.4	62.7
Qwen3-1.7B-Base	2.03B	72.9	47.0	77.9	74.7	47.6	64.2	43.3	62.4	61.3

In smaller models, MobileLLM-R1 is not explicitly optimized for the common-sense reasoning benchmarks, which explains why SmolLM attains higher performance in this regime. In the 400M–1B parameter range, MobileLLM-R1 outperforms Qwen models and Gemma-3-1B. It is important to note that these common-sense reasoning benchmarks primarily evaluate factual, social, or physical commonsense understanding rather than tasks requiring extended chain-of-thought reasoning.